

# Theory of Supersolids beyond Mean-Field

A. Stoffel and M. Gulácsi

*Max-Planck-Institute for the Physics of Complex Systems, D-01187 Dresden, Germany*  
*Nonlinear Physics Centre, Australian National University, Canberra, ACT 0200, Australia*

(Dated: November 3, 2018)

We investigate the newly discovered supersolid phase by solving in random phase approximation the anisotropic Heisenberg model of the hard-core boson  $^4\text{He}$  lattice. We include nearest and next-nearest neighbor interactions and calculate exactly all pair correlation functions in a cumulant expansion scheme. We describe the properties of the normal solid and supersolid phases and argue that based on analogies to the fermionic half filled extended Hubbard model the supersolid state corresponds to a bond-ordered-wave.

PACS numbers: 05.30.Jp, 67.80.-s, 67.80.bd, 75.10.Jm

Owing to its theoretical and experimental importance, the observation [1] of non-classical rotational inertia associated with co-existing solid and superfluid (SF) phases generated a lot of experimental controversy [2, 3] and theoretical debates [4, 5, 6]. However, the latest measurements [2] clearly show that there is an actual supersolid (SS) phase. Ref. [2] poses serious limitations for previous theories [4, 5] but simultaneously open the door for systematic theoretical approaches, which is the goal of the present Letter.

Since the work of Penrose and Onsager [7] it has been known that the SS has to exhibit simultaneously two types of order, namely diagonal long-range order (DLRO) associated with the periodic modulation in a crystal and the off-diagonal long-range order (ODLRO) associated with the phase order in the condensate. Well-known for fermionic systems such as *excitonic insulators* [8], but, for bosons the difficult reconciliation of such puzzling behavior has been debated since the late 1960's [9, 10]. After Kim and Chan's [1] discovery however, only two kinds of theoretical approaches have been pursued, namely numerical simulations [4] and phenomenological descriptions [5, 6], while many-body theories, following the pioneering works of Matsuda and Tsuneto; Liu and Fisher [10], have been completely neglected.

In this Letter we fill this gap, presenting a theory beyond the mean-field of SS. We use a cumulant expansion and solve the RPA equations for the Green's functions, taking into account the pair correlations rigorously. We will clarify the controversy over the role of the vacancies and defects, which have long been proposed to have a crucial role in the formation of a SS phase. We find that vacancies and interstitials are present even at zero temperature in the SS phase, both condense and SS may be regarded as a bond-ordered-wave as it exhibits alternating strength of the expectation value of the kinetic energy term on bonds. Also, our model confirms that the SF to SS transition is triggered by a collapsing roton minimum; however, the SS phase is stable against spontaneously induced superflow.

The quantum lattice gas (QLG) model as given by

Matsubara and Matsuda [12] is  $K = H_{QLG} - \mu N$ , with

$$K = \mu \sum_i n_i + \sum_{i,j} u_{ij} (a_i^\dagger - a_j^\dagger)(a_i - a_j) + \sum_{i,j} V_{ij} n_i n_j, \quad (1)$$

where the indices  $i$  and  $j$  run over all lattice sites,  $u_{ij}$  are the nearest and next nearest neighbor hopping parameters and  $V_{ij}$  takes nearest and next nearest two particle interactions into account. The creation and annihilation operators  $a_i^\dagger$  and  $a_i$  represent hard core bosons, i.e.,  $^4\text{He}$ -atoms. Originally, Eq. 1 was used for SF [12] and later [10] to study the possible coexistence of DLRO and ODLRO for SS. We start from a bcc lattice, which we separate into two sub-lattices, see, Fig. 1 **a**), establishing a natural way to define DLRO of solids: sub-lattice  $A$  represents the  $^4\text{He}$  ions, while sub-lattice  $B$  the interstitial centers. A normal solid (NS) then is given by a fully occupied sub-lattice  $A$ , while in a liquid phase the occupation number on both  $A$  and  $B$  sub-lattices are equal.

Conventional techniques of quantum field theory are not applicable to the QLG model due to the lack of Wick's theorem for hard-core bosons. Therefore we take advantage of the well known 1-to-1 correspondence with spin-1/2 models imposed by the following identities:  $a_j^\dagger = S_j^x - iS_j^y$ ,  $a_j = S_j^x + iS_j^y$  and  $n_j = 1/2 - S_j^z$ . This mapping is exact and transforms the QLG model to an anisotropic Heisenberg model (AHM) in an external field:

$$H = h^z \sum_i S_i^z + \sum_{i,j} J_{ij}^\parallel S_i^z S_j^z + \sum_{\alpha=x,y} \sum_{i,j} J_{ij}^\top S_i^\alpha S_j^\alpha, \quad (2)$$

where  $J_{ij}^\parallel = V_{ij}$ ,  $J_{ij}^\top = -2u_{ij}$ ,  $h^z = -\mu + \sum_j J_{ij}^\top - \sum_j J_{ij}^\parallel$ . These  $J$ 's have to be specific for  $^4\text{He}$ . The interactions between the  $^4\text{He}$  atoms are controlled by van der Waals forces and their repulsive nature at very short distances determines negative nearest neighbor interaction  $J_1^\parallel$ , evoking AF ordering in the spin language. The corresponding Lennard-Jones potential is short ranged and therefore it is sufficient [10] to only consider nearest and next nearest neighbor interactions. Hence,  $J_1^\parallel =$

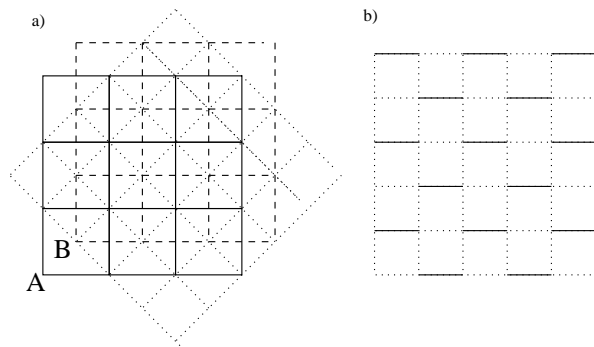


FIG. 1: **a)** A bcc lattice consists of two interpenetrating sc sub-lattices,  $A$  (continuous line) and  $B$  (long-dashed line). For simplicity we only draw the two dimensional case. In order to connect our result to the known bond-ordered-wave structures, we reduced the bcc lattice into a sc lattice (dotted line) by unfolding the Brillouin zone. **b)** The obtained bond-order-wave in the  $[100]$  direction is shown. The continuous (dashed) lines the calculated expectation values are higher (lower).

$-q_1 J_{i \in A, j \in B}^{\parallel}, J_2^{\parallel} = -q_2 J_{i \in A, j \in A}^{\parallel}, J_1^{\top} = -q_1 J_{i \in A, j \in B}^{\top}$  and  $J_2^{\top} = -q_2 J_{i \in A, j \in A}^{\top}$  where  $q_1 = 6$  and  $q_2 = 8$  are the number of nearest and next nearest neighbors on the bipartite bcc lattice. For  ${}^4\text{He}$  we will use [10],  $J_1^{\top} = 1.4K$ ,  $J_2^{\top} = 0.5K$ ,  $J_1^{\parallel} = -3.8K$  and  $J_2^{\parallel} = -1.7K$ . The results do not change if the  $J^{\parallel}$ 's are within  $\pm 2$  range of these values and  $J_B^{\parallel} > J_A^{\parallel}$ ,  $J^{\top}$ 's values remain positive. Different values of the  $J$ 's will lead more/less robust SS phase, i.e., the SS phase will occupy a larger/smaller area in the global phase diagram of  ${}^4\text{He}$ .

The ferromagnetic (FE) and anti-ferromagnetic (AF) phases do not exhibit any off-diagonal long range order: they correspond to the normal fluid and NS states of QLG, respectively. The remaining two phases of AHM are the canted ferromagnetic (CFE) and canted anti-ferromagnetic (CAF) states. As the spins in the canted phases are tilted there exists a non-vanishing transversal component, i.e.,  $\langle a_i \rangle$  is non-zero. This is the usual order parameter for SF; hence CFE corresponds to SF and CAF corresponds to the SS phase, respectively.

The Heisenberg model has been studied thoroughly although there exist only classical mean-field solutions for the CFE and CAF [10]. We solve the equation of motion in RPA to calculate the time-temperature-dependent Green's function  $G_{ij}^{xy}(t)_{Ret/Adv} = \mp i \theta(\pm t) \langle [S_i^x(t), S_j^y] \rangle$ , for all four phases. In order to preserve pair correlations as accurately as possible, we have chosen a cumulant decoupling scheme to approximate higher order Green's functions. This is the first time that a thorough cumulant RPA many-body calculation is solved for the QLG and/or AHM model and as such it represents a vital step in the understanding of these models and their phenomena.

The cumulant decoupling is based on the assumption that the last term of the equality  $\langle \hat{A} \hat{B} \hat{C} \rangle = \langle \hat{A} \rangle \langle \hat{B} \hat{C} \rangle$

$+ \langle \hat{B} \rangle \langle \hat{A} \hat{C} \rangle + \langle \hat{C} \rangle \langle \hat{A} \hat{B} \rangle - 2 \langle \hat{A} \rangle \langle \hat{B} \rangle \langle \hat{C} \rangle + \langle (\hat{A} - \langle \hat{A} \rangle)(\hat{B} - \langle \hat{B} \rangle)(\hat{C} - \langle \hat{C} \rangle) \rangle$  is small and thus negligible [13]. By using this we calculate exactly all the pair correlations. This decoupling scheme couples six Green's functions, one for each spin component in  $x$ ,  $y$  and  $z$  direction on the two sub-lattices respectively, to a set of six equations. Due to the enormous number of terms (1024 in total) within these Green's functions we do not intend to reproduce their exact form. It can be shown or alternatively argued that the Goldstone theorem of gapless modes imposes an additional condition [14] on the mean fields in the SS (and SF) phase, reducing the number of order-parameters by two. As this condition does not apply to the NS phase their Green's functions are structural different.

In the next step we calculate the phase diagram of AHM and derive all thermodynamic quantities, e.g., the pressure, the entropy and the specific heat; which are of particular interest. Note that, by fixing the  $J$ 's, the chemical potential,  $\mu$ , remains the only variable in the model, which we use as a fitting parameter. This is a natural choice as  $\mu$  is related to the pressure; they are inversely proportional. In order to derive a rigorous relationship between these two parameters we note that  $\Theta_{QLG} - \mu N = \Theta_{AHM}$ , where  $\Theta$  is an arbitrary potential, e.g., the Gibb's free energy. Then the Maxwell equation gives the desired relationship  $(\partial p / \partial \mu)_{T, V} = (\partial N / \partial V)_{T, \mu} = N_0(1 - \epsilon) / V$ , where  $N$  and  $N_0$  denotes the number of particles and lattice sites, respectively. Here we take into account explicitly the net vacancy density,  $\epsilon$ , as it has been long proposed that vacancies and defects may play a crucial role in the formation of the SS phase.

The net density of vacancies i.e. the number of vacancies minus the number of interstitials:  $\epsilon = 1 - n_A - n_B = \langle S_A^z \rangle + \langle S_B^z \rangle$ , when taken as the measure of incommensuration has been recently proposed [6] as the key parameter to characterize quantum crystals. Existing numerical calculations could only follow individual atoms [4] and as such found very difficult to pick out the effects of the density of vacancies. But this is not the case in our many-body RPA approach. In this Letter we investigate for the first time the effects of  $\epsilon$  on quantum solids in general and SSs in particular.

In order to understand the physical origin of the different phases of the QLG model, we study first the quantum fluctuation at  $T = 0$ . In previous approaches [10] such an analysis was impossible to perform as the total spin magnitude always is locked in, or restricted to the vicinity of total spin  $1/2$ . However, in our case the short and long-range correlations are taken into account by the cumulant expansion; we can explicitly see the quantum fluctuations at  $T = 0$ . In Fig. 2 we plotted the magnitude of the total spin and the angle of the spin relative to the  $x - y$  - plane as a function of the external magnetic field  $h^z$ . At large  $h^z$  ( $\mu$ , or small pressure) the AHM model is locked into a ferromagnetic phase;  ${}^4\text{He}$  is a normal liquid. There is no competition between  $S_A^z$  and  $S_B^z$

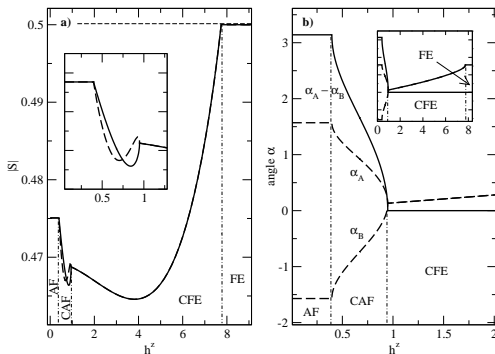


FIG. 2: The magnitude of the total spin on site  $A$  and  $B$  and the relative angle  $\alpha_{A/B} = \tan^{-1}(\langle S_{A/B}^z \rangle / \langle S_{A/B}^x \rangle)$  is plotted at  $T = 0$  in **a**) and **b**), respectively. In **a**)  $|S_A|$  and  $|S_B|$  are identical except for the SS (canted anti-ferromagnetic) phase. In **b**) the individual  $\alpha$ 's are plotted (long dashed line) and their differences (continuous line).

and the magnitude of the total spin is always  $1/2$ , i.e., a fully polarized state appears for any  $h^z$ .

As  $h^z$  ( $\mu$ ) is lowered (increasing the pressure), the contribution of the transverse term  $S_i^x S_j^x + S_i^y S_j^y$ , where  $i, j = A, B$ , increases until  $\langle S_{A/B}^x \rangle$  and  $\langle S_{A/B}^y \rangle$  become non-zero, giving rise to ODLRO. Consequently  $\langle S_{A/B}^z \rangle \neq 1/2$ . This is the well-known  $\lambda$  transition, where a fully polarized FE phase becomes canted. From Fig. 2 we can see that the magnitude of the spin is a smooth function of  $h^z$  while the relative angle between the  $A$  and  $B$  spins is still vanishing, i.e., there is still no competition between the  $A$  and  $B$  sites. In the language of the QLG model, the emergence of the CFE phase means  $n_A = n_B \neq 0$  and, being at  $T = 0$ , condense. This is the well-known SF phase and hence we do not go into further detail but merely emphasize that within the AHM description SF appears as a competition between  $h^z S_{A/B}^z$  and the transverse coupling,  $S_{A/B}^x S_{A/B}^x + S_{A/B}^y S_{A/B}^y$ .

As we further lower  $h^z$  ( $\mu$ ), i.e., as we increase the pressure,  $h^z S_{A/B}^z$  starts to compete with the Ising coupling,  $S_{A/B}^z S_{A/B}^z$  within the already well developed ODLRO. This competition leads to the CAF (SS) phase, where  $J^{\parallel}$  dominates over the effects of the external magnetic field. From Fig. 2 we can see that the magnitude and relative angle of the  $A$  and  $B$  spins differ. The relative angle variation gives the CAF phase, while the difference in their magnitude is responsible for the non-zero net density of vacancies.  $n_{A/B} = 1/2 - \langle S_{A/B}^z \rangle$ , Fig. 2 implies that  $0 \leq n_A \leq 1/2$  and  $1/2 \leq n_B \leq 1$  in the SS phase. Hence, as we increase the pressure, there will be a density transfer from the vacancies to the interstitial sites, i.e.,  $n_A \rightarrow n_B$ . This particle density transfer is induced by the increasing strength of pair correlation  $\langle S_A^z S_B^z \rangle$  and it only happens in the SS phase; hence it stands as the key in understanding the origin of this phase. Within the QLG model, this effect will result in an alternating

strength of the expectation value of the kinetic energy term on the bonds. This dimer order is called a bond-order-wave (BOW) in the half filled fermionic extended Hubbard models [15]. Calculating the expectation value of the kinetic energy of the QLG model we plot the [100] BOW corresponding to SS, see Fig. 1 **b**). Similar BOWs appear also in [010] and [001] corresponding to the roton minima (see below). Hence, we conclude that the boson condensation phenomenon of SS is a BOW.

Since the 1970's [11], it has been suggested that a SS transition might be triggered by a collapsing roton minimum. In our approach we could verify this for the first time and found that the excitation spectrum indeed goes soft at [100] ([010] and [001]) at the SF to SS transition. This is true for input parameters which satisfy  $J_1^{\top} + J_2^{\top} + J_1^{\parallel} - J_2^{\parallel} < 0$ . In all these cases the spectrum is not effected in the [111] direction. There are situations when the roton minimum collapses at [111] instead of [100], namely for  $-2J_2^{\top} / (J_1^{\top} + J_2^{\top} + J_2^{\parallel}) > 0$ . However, these cases induce structural instability and refer to a transition to a different state.

It was also conjectured [11] recently that the SF phase in the vicinity of the SF to SS transition is unstable against spontaneously induced superflow and superflow associated with vortices. This can be easily shown not to be true in our RPA approach. A net superflow is either given by a moving condensate which results in a gradient of the phase of the wave-function or equivalently by a moving environment while the condensate stays at rest. Using the latter, we add to Eq. (1) the term,  $\int d^3x \psi^{\dagger}(x)(i\hbar \mathbf{v}_{\mathbf{n}} \cdot \nabla)\psi(x)$  which transformed into the AHM language gives an additional contribution  $\sum_{ij} J_{ij}^{\times} (S_i^x S_j^y - S_j^x S_i^y)$  to Eq. (2). Here the nearest and next-nearest neighbor cross coupling constants are anti-symmetric ( $J_{ij}^{\times} = -J_{ji}^{\times}$ ) and are zero for directions perpendicular to the motion of the environment  $\mathbf{v}_{\mathbf{n}}$ . Calculating the excitation spectrum it is noticed that even though  $J^{\times}$  gives a small contribution to the spectrum, it does not influence the roton dip that triggers the SF to SS transition.

At finite temperature we analyze the NS to SS transition first, as this is known experimentally [1]. At constant chemical potential, the NS to SS transition is of second order with a discontinuity in the net vacancy density. In Fig.3 **a**) we show a typical curve of the net vacancy density at constant chemical potential. We have chosen a value for the chemical potential corresponding to a pressure just above the critical pressure measured by Kim and Chan [1]. The discontinuity in  $\varepsilon$  is suggestive for a commensurate-incommensurate transition, when the net vacancy density is taken as a measure of incommensuration, as it is done in Ref. [6].

The thin dashed curves in Fig.3 **a**) show what the net vacancy density would be if a SS phase would not appear: at  $T \rightarrow 0$  the ground state is a perfect, commensurate

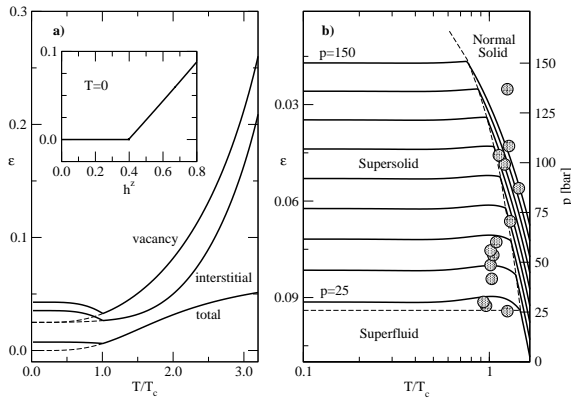


FIG. 3: **a)** Net vacancy density at the NS to SS transition for fixed  $h^z$ . The dashed curves are what the net vacancy density of the normal crystal would be without SS. Inset shows the  $T = 0$  limit as a function of  $h^z$ . **b)** Net vacancy density of  ${}^4\text{He}$  (left axis) for different values of pressure (right axis) superimposed onto Kim and Chan's [1] phase diagram (filled circles).

crystal, i.e., a Mott insulator, which is not a SF. In NS the density of vacancies increases faster than that of interstitials with increasing temperature, as reported in Ref.[16], indicating that thermal fluctuations favor vacancies more than interstitials. This is not the case for the SS phase, where all three  $\varepsilon$ 's have the same mean-field SF form:  $\varepsilon_0(1 - \sqrt{\Delta/k_B T}) \exp(-\Delta/k_B T)$ . Here,  $\varepsilon_0 \equiv \varepsilon(T = 0)$ , shown in the inset of Fig.1 **a)**, shows that the SS phase is driven by the chemical potential, similarly to a correlation driven Mott transition:  $\varepsilon_0 \propto (\mu - \mu_c)$ , where the proportionality constant for our model is  $(\langle S_A^x \rangle / \langle S_B^x \rangle)$ .

Recalculating the NS to SS transition as a function of the pressure and superimposing it onto the known phase diagram [1], we obtained Fig.1 **b)**. It shows a very good fit to the experimental points. For these isobar curves, as it can be seen, the net vacancy density is constant in the SS phase. This is because the thermal expansion of the SS phase is evanescently small.

In conclusion, we have shown that the transition into a SS phase is of the incommensurate-commensurate type with properties suggesting a BOW. The AHM model in RPA does explain most of available experimental data of the SS  ${}^4\text{He}$  phase, which we will present in a future publication. Due to the interest in the recent experiments of Aoki, et al., [2], we briefly outline the solution to Ref.[2] based on Eq. 2. As we have shown, the SS of  ${}^4\text{He}$  is a true solid hence, the underlying lattice is the reference frame. In torsional oscillator measurements, however, the reference frame is accelerated. Hence, the kinetic energy will acquire a new cross-coupling term, as presented earlier:  $J^{\times} a \sum_{i,j} (S_i^x S_j^y - S_j^x S_i^y)$ , where  $a$  is the acceleration. This will contribute with  $J^{\top} \sum_{i,j} \cos(\phi_i - \phi_j + J^{\times} / J^{\top} a)$  to the vortex dynamics. This implies that the motion of a single vortex/antivortex is given by  $d\mathbf{r}_v/dt \propto$

$\pm \boldsymbol{\Omega} \times d\mathbf{v}_n/dt$ , rather than the well-know SF equation  $d\mathbf{r}_v/dt \propto \pm \boldsymbol{\Omega} \times \mathbf{v}_n$ , where  $\mathbf{v}_n = \mathbf{r} \times \boldsymbol{\Omega}$  is the velocity of the rotating cylinder  $\boldsymbol{\Omega} = \Omega_0 \cos(\omega t)$ . Thus, for a SS the signal  $\rho_s/\rho$  is independent of the frequency as seen in the Aoki, et al., experiments [2], i.e., the acceleration and not the rim velocity is the defining parameter in the motion of vortices.

- 
- [1] E. Kim and M.H.W. Chan, Nature **427**, 225 (2004); Science **305**, 1941 (2004).
  - [2] A. Penzev, Y. Tasuta and M. Kubota, J. Low Temp. Phys. **148**, 677 (2007); M. Kondo, S. Takada, Y. Shibayama and K. Shirahama, J. Low Temp. Phys. **148**, 695 (2007); Y. Aoki, J.C. Graves and H. Kojima, cond-mat/0705560; J. Day and J. Beamish, cond-mat/0709.4666; E. Kim, et al., cond-mat/0710.3370.
  - [3] A.S.C. Rittner and J.D. Reppy, Phys. Rev. Lett. **97**, 165301 (2006); *ibid.* **98**, 175302 (2007); S. Sasaki, et al., Science **313**, 1098 (2006).
  - [4] D.M. Ceperley, B. Bernu, Phys. Rev. Lett. **93**, 155303 (2004); N. Prokof'ev, B. Svistunov, Phys. Rev. Lett. **94**, 155302 (2005); D.E. Galli, M. Rossi and L. Reatto, Phys. Rev. B **71**, 140506(R) (2005); E. Burovski, et al., Phys. Rev. Lett., vol. 94, p. 165301 (2005); M. Boninsegni, et al., Phys. Rev. Lett. **97**, 080401 (2006); **96**, 105301 (2006); B.K. Clark and D.M. Ceperley, Phys. Rev. Lett. **96**, 105302 (2006).
  - [5] W.M. Saslow, Phys. Rev. B **71**, 092502 (2005); Xi Dai, et al., Phys. Rev. B **72**, 132504 (2005); A.T. Dorsey, et al., Phys. Rev. Lett. **96**, 055301 (2006); Jinwu Ye, Phys. Rev. Lett. **97**, 125302 (2006).
  - [6] P.W. Anderson, W.F. Brinkman and D.A. Huse, Science **18 Nov. 2005**; **310**: 1164; P.W. Anderson, Nat. Phys. **3**, 160 (2007).
  - [7] O. Penrose and L. Onsager, Phys. Rev. **104**, 576 (1956).
  - [8] A.M. Gabovich and A.I. Voitenko, Low Temp. Phys. **26**, 305 (2000).
  - [9] A.F. Andreev and I.M. Lifshitz, Sov. Phys. JETP **29**, 1107 (1969); L. Reatto, Phys. Rev. **183**, 334 (1969); G.V. Chester and L. Reatto, Phys. Rev. **155**, 88 (1967); G.V. Chester, Phys. Rev. **A2**, 256 (1970); A.J. Leggett, Phys. Rev. Lett. **25**, 2543 (1970).
  - [10] H. Matsuda and T. Tsuneto, Prog. Theor. Phys. Suppl. No. 46, 411 (1970); K.-S. Liu and M.E. Fisher, Jour. Low Temp. Phys. **10**, 655 (1973).
  - [11] T. Schneider and C. P. Enz, Phys. Rev. Lett. **27**, 1186 (1971); E. Zhao and A. Paramekanti, Phys. Rev. Lett. **96**, 105303 (2006).
  - [12] T. Matsubara and H. Matsuda, Prog. Theor. Phys. **16**, 569 (1956); H. Matsuda and T. Matsubara, *ibid.* **17**, 19 (1957).
  - [13] P.E. Bloomfield and E.B. Brown, Phys. Rev. B **22**, 1353 (1980).
  - [14] P.E. Bloomfield and N. Nafari, Phys. Rev. A **5**, 806 (1972).
  - [15] For a review, see M.-A. Ozaki, Int. J. Quantum Chem. **42**, 55 (1992).
  - [16] B.A. Fraass, P.R. Granfors and R.O. Simmons, Phys. Rev. B **39**, 124 (1989).